



Silver nanoparticles engineered by thermal co-reduction approach induces liver damage in Wistar rats: acute and sub-chronic toxicity analysis

Nandita Dasgupta^{1,2} · Shivendu Ranjan³ · Chidambaram Ramalingam¹ · Mansi Gandhi⁴

Received: 3 October 2018 / Accepted: 23 February 2019 / Published online: 6 March 2019
© King Abdulaziz City for Science and Technology 2019

Abstract

Recently, nanotechnology applications have increased tremendously in consumer products. However, it has been observed that these nanoparticles can cause a potential risk to the environment as well as human health. In the present manuscript, we have analyzed acute and sub-chronic toxicity of engineered silver nanoparticles (AgNPs) by assessing the impact on Wistar rats. AgNPs were synthesized by a novel approach—thermal co-reduction—with spherical shape and a uniform size distribution of 60 nm. The estimated LD₅₀ value was observed to be more than 2000 mg/kg bw in acute toxicity studies. Sub-chronic toxicity indicated impairment of liver and kidney enzymes and various hematological and biochemical parameters. Tissue distribution studies indicated the target organ for accumulation is liver after treatment with AgNP. Particle deposition and congestion was observed in major organs-though, and heart and pancreatic tissues were not affected even by the higher doses. On the basis of the observations of this study, it is concluded that up to 40 mg/kgbw is a safer dose of AgNPs (60 nm, engineered by thermal co-reduction approach) and further research will be required to validate the long-term accumulation in body. In addition, it can also be considered by policymakers for the safer use of AgNPs.

Keywords Thermal co-reduction approach · Silver nanoparticle · Wistar rats · Acute toxicity · Sub-chronic toxicity · Histopathology

Introduction

Nanomaterials possess unique properties which differ from their bulk counterparts largely with respect to their large surface-to-volume ratio (Ma et al. 2010). AgNPs have been used in a range of marketed products, i.e., from food, electronics,

drugs, biomedical devices, imaging technology, etc. This wide range of products makes it of utmost importance to analyse its toxic properties. Since nanoparticles have greater penetration property than their bulk counterparts, the toxicity of these particles is expected to be greater. Wherein, AgNPs are reported to be cytotoxic in nature. Several reports have indicated that these nanoparticles can induce oxidative stress and ROS leading to membrane and DNA damage. This structural damage leads to apoptosis or genetic alteration in cells, thus affecting the overall health being of the organism (Kim et al. 2009a).

Since the toxicity of AgNPs directly depends upon the synthesis protocol followed; different toxicity data are reported in the literature. Size and particle coating also affects the toxicity of AgNPs. It is still not known the extent to which AgNPs undergo changes in the digestive tract. Changes in size and morphology of AgNPs in simulated gastric and intestinal fluids are observed, but the degree of breakage or clumping is not known (Pindáková et al. 2017). The major mechanism of action is predicted to be generation of non-specific reactive oxygen species (ROS). The

✉ Shivendu Ranjan
shivenduranjan@gmail.com

¹ Nano-food Research Group, Instrumental and Food Analysis Laboratory, Industrial Biotechnology Division, School of BioSciences and Technology, Vellore Institute of Technology, Vellore, Tamil Nadu, India

² Department of Biotechnology, Institute of Engineering and Technology, Dr. APJ Abdul Kalam Technical University (Formerly Uttar Pradesh Technical University), Lucknow, Uttar Pradesh 226021, India

³ Faculty of Engineering and the Built Environment, University of Johannesburg, Johannesburg, South Africa

⁴ School of Advanced Sciences, Vellore Institute of Technology, Vellore, Tamil Nadu, India

structural injury or damage of mitochondria can also release excessive ROS. This oxidative stress leads to undergo apoptosis in cells (Aker et al. 2018; Alarifi et al. 2017). Exposure of AgNPs to *C. elegans* leads to increased heat-shock protein expression, an indication of endoplasmic reticulum stress, but the exact mechanism of action for apoptosis is not clear (Srivastava et al. 2012).

Due to the wide range of products in which AgNPs are used, they are either directly ingested or through environmental contamination. They can enter through several routes of exposure such as through gastrointestinal or respiratory system and reach the blood or major organs. There are also concerns that AgNPs can pass through blood–brain barrier (BBB) by transcytosis of capillary endothelial cells or into other tissues and inducing further damage (Tang et al. 2010). Thus, it is necessary to have a better understanding on the long-term effects of AgNPs on various biological systems (Dobrzyńska et al. 2014). In our earlier work, we have engineered AgNP with a novel thermal co-reduction approach and have analyzed the microbial as well as cellular toxicity including the mechanism of action on microbes (Dasgupta and Ramalingam 2016). This engineered AgNP has also been studied for its interaction with biomolecules such as proteins and enzyme, hence provides an insight into how these particles will interact within the body; if ingested intentionally or unintentionally (Dasgupta et al. 2016). In this study, we investigated the effects of AgNPs on Wistar rats. The acute and sub-chronic toxicity was observed for different concentrations. The effect was observed for liver and kidney enzymes which give a direct correlation between hepatic injury and toxicity. The enzymes such as ALP, AST, ALT and GGTP and histopathological changes were observed.

Materials and methods

Chemicals

Analytical grade reagents were used throughout the experiment and no further purification was performed. Double deionized (DI) water (with a measured resistivity of 18.2 MΩ/cm) was used, throughout the procedures. The enzymatic kits were procured from M/s Agappe Diagnostics Ltd., India.

AgNP engineering and characterization

Silver nanoparticles were engineered by our earlier standardized novel approach, i.e., ‘thermal co-reduction approach’ (Dasgupta et al. 2016). Furthermore, characterization data for UV–Vis spectrophotometer (AU2701, Systronics Inc., India), X-ray diffractometer (D8 Advance Model,

Bruker, Germany), scanning electron microscope (SEM), Energy-Dispersive Spectroscopy (EDAX) (JEOL JSM-7600F, Japan), transmission electron microscopy (TEM) (JEOL JEM 2000Fx II, Japan, at 200 kV), dynamic light scattering (DLS) (HORIBA Instruments Pvt Ltd., Singapore), zeta potential, and atomic force microscope (AFM) (Model-Nanosurf easyscan 2 AFM, Switzerland) were done to estimate size and shape of the nanoparticle (Dasgupta et al. 2016). The nanoparticle obtained was of 60 nm and spherical in shape. The toxicity analysis was done as discussed below.

Animal model for in vivo study

Once after getting the due approval and clearance of Institutional animal ethics committee (IAEC NO: VIT/IAEC/12/July23/6), the animal experiments were performed at the institute’s animal house. For the present study, female Wistar rats of 6–8 weeks and 130–150 g in weight were chosen. Animals were maintained on standard pellet feed and water ad libitum. Guidelines of Committee for the Purpose of Control and Supervision on Experiments of Animals (CPCSEA), Government of India were strictly followed for carrying out the in vivo experiments. The rats were weighed and divided in treatment groups, such that the average weight of body in each group was similar.

Treatment of animals with AgNP

The animals were first observed for acute toxicity as a preliminary reference for dose selection. According to the OECD test guideline 420, when the test material toxic impact is not known, then a limit dose of 2000 mg/kg bw should be taken for acute toxicity studies (OECD test guideline 420). AgNPs were gavaged (0.2 ml) as an aqueous suspension. The experimental design included four groups with three different doses (500 mg/kg bw, 1000 mg/kg bw, and 2000 mg/kg bw) and a control group. The study was carried out for 14 days and 5 animals per group. For the first 6 h after dosing, mortality checks and clinical observation were conducted once per hour and further once daily for 14 days. Measurement of body dose was performed on treatment day and further on test days 1, 7, and 14.

If no acute toxicity observed-limit dose of 1000 mg/kg bw can be used as higher dose level in sub-chronic studies (OECD, 1998 guidelines). Based on literature survey, the limit dose for sub-chronic studies, 100 mg/kg bw was chosen. AgNPs were orally administered as an aqueous suspension. The experimental design included six groups with five different doses (20 mg/kg bw, 40 mg/kg bw, 60 mg/kg bw, 80 mg/kg bw, and 100 mg/kg bw) and a control group. The study was carried out for 12 weeks and 5 animals per group. The rats were then analyzed for different parameters

as discussed further. Mortality checks and clinical signs were analyzed daily and further body weight was recorded on weekly basis, during the study period (Yun et al. 2015).

Body weights, feed, and water consumption and clinical signs

Clinical signs such as changes in fur, skin, nasal secretions (mucus and bleeding), mucous membranes and eyes, incidence of secretions and excretions, autonomic activity such as tear secretion (lacrimation), fur erection (piloerection) and unusual pattern for respiration were examined daily. Rats were also observed for any unusual changes in locomotion, gait, posture, handling response, repetitive circling, or bizarre behavior such as self-mutilation, walking backward, etc. Body weights, feed, and water intake were examined on the treatment day and further on test days 1, 7, and 14 for acute toxicity study. While for sub-chronic study, body weights, feed, and water intake were measured once before treatment and then at weekly intervals (Ranganathan et al. 2016).

Biochemistry panel analysis

At the end of the study, for both acute as well as sub-chronic, all the rats were anesthetized with ketamine (22–24 mg/kg bwim) and further cervical dislocation method was followed for sacrificing. Cardian puncture approach was adopted to collect total blood and was analyzed further for various enzymatic assays such as total bilirubin, alkaline phosphatase (ALP), aspartate aminotransferase (AST), alanine transaminase (ALT), and γ -glutamyltranspeptidase (GGTP). The enzymatic and protein assays were performed as per the instructions provided by M/s Agappe Diagnostics Ltd., India. Various other biochemical parameters were also observed such as albumin (ALB), cholesterol (CHO), creatinine (CRE), glucose (GLU), lactatedehydrogenase (LDH), total protein (TP), inorganic phosphorous (IP), triglyceride (TRG), sodium (Na), and potassium (K). Hematology was analyzed for erythrocyte count (RBC), total leukocyte count (WBC), hemoglobin (HGB), mean corpuscular hemoglobin (MCH), mean corpuscular hemoglobin concentration (MCHC), platelets (thrombocytes) count (PLT), mean corpuscular volume (MCV), hematocrits (HCV), lymphocytes (LYO), red cell distribution width (RDW), neutrophils (NEU), monocytes (MONO), eosinophils (EOS), basophils (BASO) hematological parameters were analyzed by and automated hematology analyzer (K-4500, Sysmex Corp., Japan). Differential counts of leukocytes were checked and examined using automatic analyzer MICRO HEG-120A (Omron Tateishi Electronics Co. Ltd., Japan).

Histopathology

At necropsy, all major tissues and organs were observed macroscopically with the caution for any lesions and were removed surgically, and further blotted after thorough wash in isotonic saline. Major organs such as liver, kidney, pancreas, heart and lungs were fixed in formalin (neutral-buffered, 10%) and stained using eosin and hematoxylin. Further study was done microscopically for any histological changes (Ranganathan et al. 2016).

Determination of engineered AgNP concentrations in tissues

Organs were weighted carefully prior to the starting the digestion of organic materials of all samples; furthermore, organs were separately soaked in nitric acid solution (a digestion solution) for 30 min; once all the organic materials were digested from the samples, the digestion solution was kept at 90 °C to evaporate the nitric acid and then thoroughly washed with 5 ml of hydrochloride acid. Ultimately, the samples were diluted with DI water to a metered volume. Engineered AgNP concentration in the digestion solution was examined by inductively coupled plasma mass spectrometry (ICP-MS, Thermo X series II). Engineered AgNP concentration of AgNP in digested tissue samples was reported as silver quantity/weight of organ (μg of Ag/g of organ) using mean \pm standard deviation (Espinosa-Cristobal et al. 2013).

Statistical analysis

One-way ANOVA was adopted for the statistical evaluation of data and expressed as mean \pm SEM. $p \leq 0.05$ was considered as significant.

Results and discussion

Engineering of AgNP and characterization

AgNPs were synthesized by thermal co-reduction approach (Dasgupta et al. 2016). The AgNPs were first analyzed by UV–visible spectrophotometer and the crystal structure was analyzed using X-ray diffractometer; further size and shape were characterized and confirmed by several sophisticated instrumentation such as DLS, AFM, SEM-EDAX, and HR-TEM. These characterization data reveal that monodispersed spherical-shaped AgNPs were synthesized of size 60 nm. Figure 1 denotes the characterization

Fig. 1 Characterization of silver nanoparticles of size **a** UV–Vis spectra ($\lambda = 382$ nm); **b** XRD graph, **c** AFM image; **d** DLS peaks, **e** SEM image, **f** EDAX image and **g** HR-TEM images (Reprint with permission from Dasgupta et al. (2016))

of monodispersed AgNP of size 60 nm with -39.4 mV as the zeta potential (Dasgupta et al. 2016).

Acute toxicity

Following oral exposure to both ionic and nanoparticulate silver suspensions, silver has been reported to be deposited as particles in tissues such as the skin epidermis, the glomeruli, and the intestines. The most well-described depositional effect is the blue–grey discoloration of the human skin that is observed during argyria (Chang et al. 2006).

In our study, acute toxicity was studied for three different doses for 14-day repeated toxicity. Mortalities were not witnessed in both the negative control rats as well as the engineered AgNP-administered rats. Thus, the acute oral LD_{50} is estimated to be more than 2000 mg/kg of body weight. There was no significant clinical observational change. Moreover, AgNPs gavaged any significant change in body weight, feed, and water intake were not observed in rats. At the end of the examination, serum was extracted from the sacrificed animals and various biochemical parameters were analyzed. It was observed that except for ALT, all the other enzymes and protein estimation were not significantly altered. As represented in Table 1, a significant increase in ALT levels was noticed which was dose dependent in nature.

Several reports indicate that short exposure to AgNP does not induce significant biochemical changes; however, accumulation of silver or silver ions has been reported. Owing to the different synthesis method, shape, and size, AgNPs are reported to have different toxicity levels. An *in vivo* toxicity experimentation was performed on Sprague–Dawley rats—orally treated for 28 days with nano-silver by Kim and his team at doses of 30, 300, and 1000 mg/kg bw per day. Notably, neither any clinical signs were detected nor any difference in consumption of food between control and treated groups. In addition, the absence of any changes in organ weight or body weight has been noticed. The impacts on biochemistry of blood, i.e., increase in the level of alkaline phosphatase and cholesterol at higher AgNP doses, showed moderate hepatotoxicity of nano-silver as similar to our study using engineered AgNP (Kim et al. 2008). Maneewattanapinyo et al. reported LD_{50} for colloidal form of nano-silver to be more than 5000 mg/kg bw. They also did not observe any acute toxic signs throughout the observation period (Maneewattanapinyo et al. 2011). Zande et al. reported that after 28-day oral exposure of AgNP, silver concentration was highest in liver and spleen regardless of the size and coating of AgNP. However, they also reported that silver

was cleared from most organs after 8 weeks postdosing, but remarkably not from the brain and testis (van der Zande et al. 2012). Lankveld et al. also observed that after injecting AgNP of different sizes (20, 80, and 110 nm), AgNPs are rapidly removed from the blood and widely dispersed to various organs (lungs, liver, spleen, kidney, brain, testes, and even heart) irrespective of the size. They reported that the 20 nm sized nanoparticledispersedlargely to liver, followed by kidneys and spleen. On the other hand, the larger sized nanoparticles dispersedlargely to spleen followed by liver and lung (Lankveld et al. 2010). Similarly, Park et al. also observed that different sizes of nano-silvers (22 nm, 42 nm, and 71 nm) are dispersed in different organs including lung, kidney, liver, brain, and even testis, on contrary, AgNP of a greater size (323 nm) cannot access. However, they also observed that the weight of the body or the organ/body weight ratio was not expressively varying between the AgNPs-treated groups and the control in a 14-day study using mice (Park et al. 2010). Thus, the previously reported literature indicates that certain biochemical parameters are not significantly altered; however, it gets accumulated in the major organs.

Sub-chronic toxicity

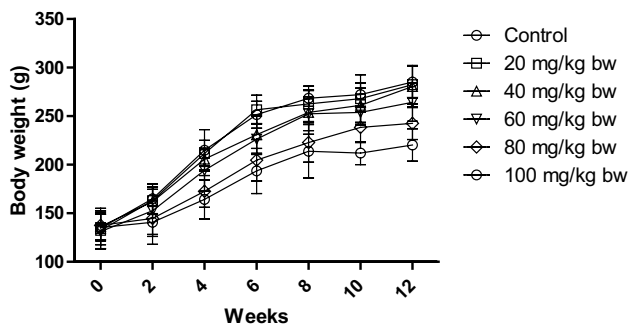
Body weights, feed, and water consumption and clinical signs

Despite the extensive use of marketed products containing AgNPs, *in vivo* toxicity data on orally ingested nano-silvers are very few (Gaillet and Rouanet 2015). *In vitro* experiments showed discrete (but not certainly mutually exclusive) toxicity mechanisms of nano-silvers, which include (1) generation of ROS, with successive oxidative stress; (2) interaction of nano-silvers with cellular enzymes and proteins due to the binding of free thiol groups with AgNPs; and (3) imitation of endogenous ions (e.g. potassium, sodium, or calcium) which further causes the disturbances at ion regulatory level (Völker et al. 2013). These mechanisms eventually cause cellular damage, cytokine production, and ultimately apoptosis. Various *in vitro* experiments have been performed to demonstrate the genotoxic as well as cytotoxic impacts of nano-silver which are dose- and size dependent, as well as cell type- and coating material-dependent (El Badawy et al. 2010; Nguyen et al. 2013; Park et al. 2011).

While comparing the general outcomes of *in vitro* studies, the *in vivo* results are contentious regarding the beginning of adverse impact after the administration of nano-silver. Few of the earlier works indicated the plausible toxic impact on intestine, liver, lung, and organs of nervous and immune systems. Such plausibility may arise either after single or repeated AgNP exposure, and further depends upon routes of exposure or administration (De Jong et al. 2013; Kim

Table 1 Acute toxicity on Wistar rats after treatment with different concentrations of AgNPs indicates dose-dependent increased levels of ALP

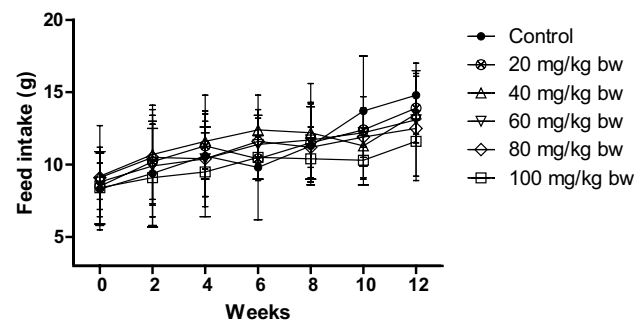
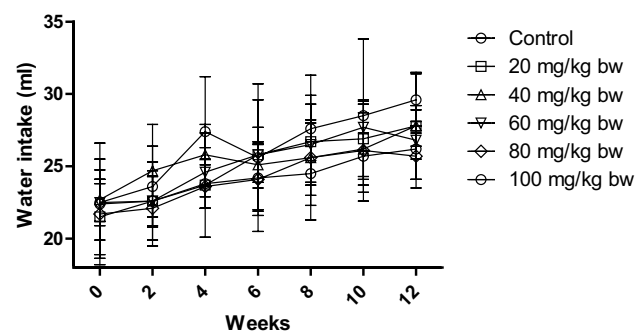
S. no.	AgNP (mg/kg bw)	ALP (U/l)
1	0 (negative control)	115.8 ± 21.4
2	500	181.9 ± 25.1
3	1000	221.1 ± 34.7
4	2000	239.1 ± 18.8

**Fig. 2** Body weight of rats after treatment with different concentrations of AgNP. The body weight of control rats increased with age, while the body weight of rats decreased after treatment with AgNP. Each datum represents the mean ± SD ($n = 5$)

et al. 2010; Park et al. 2010; Shahare et al. 2013; Sung et al. 2009; Xue et al. 2012). Though, few studies observed even absence of any relevant adverse impacts (Hadrup et al. 2012; Stebounova et al. 2011; van der Zande et al. 2012). Such contradiction in results maybe due to the high variations of the tested nano-silvers, with respect to the source (commercially available or synthesized in laboratory), shape, size, coating material, dispersion state, as well as concentration (i.e., AgNP number and silver mass). In addition, the species of test animals, age, sex, strain, as well as the complete experimental design (exposure time, dose, and end-sampling points) might have the effect on the final outcome of the in vivo experimentations.

In our study, the sub-chronic toxicity study was carried for 12 weeks. During this study, no mortality or treatment-related abnormal clinical symptoms were observed. However, there was a significant reduction in body weight, feed, and water intake for the higher dose group. As depicted in Fig. 2, the weight of the control rats increased from 134.6 ± 5.3 to 285.1 ± 16.7 g with the age. However, the higher dose group significantly decreased body weight to 242.7 ± 16.8 and 220.3 ± 16.6 as compared to control for 80 mg/kg bw and 100 mg/kg bw, respectively.

Similarly, as depicted in Figs. 3 and 4, the feed and water intake decreased for the higher doses only, but the reduction was not significant as compared to control. The

**Fig. 3** Feed intake of rats after treatment with different concentrations of AgNP. The feed intake of control rats increased with age, while the feed intake of rats decreased after treatment with AgNP. Each datum represents the mean ± SD ($n = 5$)**Fig. 4** Water intake of rats after treatment with different concentrations of AgNP. The water intake of control rats increased with age, while the water intake of rats decreased after treatment with AgNP. Each datum represents the mean ± SD ($n = 5$)

feed intake decreased to 12.5 ± 1.6 g and 11.6 ± 0.3 g for 80 mg/kg bw and 100 mg/kg bw, respectively, as compared to control which was 14.8 ± 1.7 g. The water intake decreased to 25.7 ± 1.6 ml and 26.2 ± 2.7 ml for 80 mg/kg bw and 100 mg/kg, respectively, as compared to control which was 29.6 ± 1.8 ml.

Shahare et al. also observed significant decrease in body weight without any difference in feed and water consumption. They observed AgNP interacts with the protective layer of the glycocalyx and other structural elements of the microvilli of the intestinal absorptive cells causing structural changes, resulting in the alteration of membrane permeability and finally destruction of the microvilli. Subsequently, the epithelial cells of gastrointestinal tract get destroyed and are the reason for the decrease in body weight of mice (Shahare et al. 2013). Similarly, Loeschner et al. also observed the presence of silver the ileal tissue principally in the form of nanometric nodules, in the lysosomes of macrophages in the lamina propria, in the basal layer of the epithelium, and in the submucosa. Thus, it indicates that AgNPs interact with the intestinal

wall and hinder with the metabolism in rats after exposure to AgNPs (Loeschner et al. 2011).

Hematology analysis

After 12 weeks of study, hematology parameters were analyzed including WBC, RBC, HGB, HCT, MCV, MCH, MCHC, PLT, LYO, RDW, NEU, MONO, EOS, and BASO. Significant changes were observed for WBC, HCT, MCV, MCHC, NEU, EOS, and BASO. Table 2 depicts the changes in hematology parameters after AgNP treatment. Most of the parameters were significantly altered for the higher doses, that is for 100 mg/kg bw treatment dose. As indicated in our study, a significant increase in WBC and a significant decrease in platelets indicate immunogenic response after treatment with AgNP (Chakraborty et al. 2016; Daniel et al. 2010; Lappas 2015). Chakraborty et al. have reported an increase in WBC, lymphocyte and granulocyte counts even at extremely low doses (2 mg/kg bw). This may be due to nanoparticle–protein complexes in biological systems can induce an abnormal unfolding of adsorbed proteins, which may result in an unwanted immune response through the exposure of hidden epitopes. This results in an unwanted immune response, and hence, an increase in WBC and lymphocytes was observed (Chakraborty et al. 2016). De Jong et al. also observed a decrease in HCT, HGB, and MCH which may be due to increased number of reticulocytes. They also observed an increase in number of blood neutrophilic granulocytes (De Jong et al. 2013). As indicated in our study, an increase in RBC count occurs after AgNP treatment. Chen et al. observed that an active uptake by RBC occurs for AgNP of size ~ 50 nm which is similar to our

average reported size that is, 60 nm. A significant increase in RBC count can be due to the uptake of AgNP by RBC (Chen et al. 2015). The alterations in the red blood cells may indicate an effect of the nanoparticles on hemoglobin syntheses during red blood cell maturation/formation in the bone marrow. The increase in reticulocytes in the blood indicates an increased possibly compensatory production of red blood cells (De Jong et al. 2013).

A probable mechanism for the significant alteration in hematology parameters could be the interaction of AgNP with biomolecules and proteins and triggers an immunogenic response with the subsequent release of cytokines and other inflammatory molecules. The AgNP particles are then accumulated in the major organs and the hematology parameters showed significant changes for the higher doses in response to the inflammation (Chakraborty et al. 2016; Park et al. 2011; Tiwari et al. 2011).

Serum biochemistry analysis for liver and kidney function

In our study, we analyzed different parameters for serum biochemistry such as ALB, CHO, CRE, GLU, LDH, TP, GLO, IP, TRG, Na, K, and certain enzymes. As depicted in Table 3, significant changes were observed for the higher doses, that is, 80 mg/kg bw and 100 mg/kg bw. AgNPs are reported to interact with serum albumin and undergo structural alteration (Dasgupta et al. 2016; Gnanadhas et al. 2013). Garza-Ocañas et al. indicate that AgNP has a greater tendency to react with sulfur- or phosphorus-containing proteins in the membrane or inside the cells and phosphorus-containing elements such as DNA. It has been suggested that the disruption of the membrane morphology may cause a

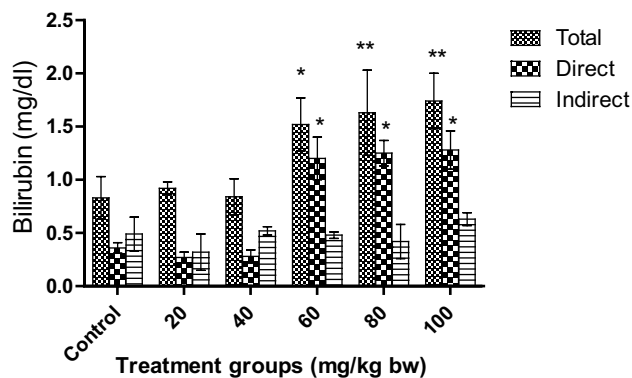
Table 2 Evaluation of various hematological parameters after exposure to different concentrations of AgNP

Hematological parameters	Dose (mg/kg bw)					
	0 (control)	20	40	60	80	100
WBC ($10^3/\mu\text{l}$)	5.58 ± 0.32	5.62 ± 0.84	5.87 ± 0.74	6.01 ± 1.05	6.22 ± 0.37	6.36 ± 0.81*
RBC ($10^6/\mu\text{l}$)	8.53 ± 0.14	8.57 ± 0.26	8.69 ± 0.42	8.83 ± 0.52	9.07 ± 0.26	9.24 ± 0.63
HGB (g/dl)	16.26 ± 0.73	16.22 ± 0.44	16.18 ± 0.53	16.11 ± 0.35	16.05 ± 0.37	15.98 ± 0.38
HCT (%)	34.52 ± 1.85	34.49 ± 1.41	34.42 ± 0.58	34.31 ± 0.83	33.95 ± 0.84	33.66 ± 0.29*
MCV (fl)	40.82 ± 1.04	40.97 ± 0.94	41.28 ± 0.74	41.57 ± 0.82	41.72 ± 0.57	41.80 ± 0.62*
MCH (pg)	19.28 ± 0.38	19.31 ± 0.48	19.38 ± 0.22	19.42 ± 0.58	19.51 ± 0.73	19.58 ± 0.52
MCHC (g/dl)	47.26 ± 1.46	47.07 ± 1.25	46.62 ± 1.51	46.27 ± 1.22	46.14 ± 1.32	45.98 ± 1.71*
PLT ($10^3/\mu\text{l}$)	770.2 ± 111.2	729.5 ± 79.4	719.4 ± 68.2	707.9 ± 79.2	695.3 ± 82.3	681.2 ± 79.6*
LYO (%)	71.36 ± 4.24	71.20 ± 2.83	70.65 ± 2.77	69.17 ± 1.43	67.92 ± 2.59	67.31 ± 2.37
RDW (%)	19.48 ± 1.58	19.41 ± 1.12	19.27 ± 2.64	19.14 ± 2.42	18.81 ± 1.58	18.62 ± 1.58
NEU (%)	24.62 ± 2.13	24.93 ± 1.49	25.24 ± 2.60	25.62 ± 1.63	26.41 ± 1.93	27.81 ± 2.63*
MONO (%)	3.02 ± 1.42	3.23 ± 1.73	3.37 ± 1.28	3.87 ± 0.96	4.14 ± 1.65	4.61 ± 1.51
EOS (%)	0.43 ± 0.09	0.38 ± 0.02	0.26 ± 0.08	0.22 ± 0.07	0.20 ± 0.08	0.17 ± 0.06*
BASO (%)	0.18 ± 0.01	0.15 ± 0.03	0.13 ± 0.02	0.09 ± 0.01	0.05 ± 0.01	0.01 ± 0.01*

*Significance of $p < 0.05$

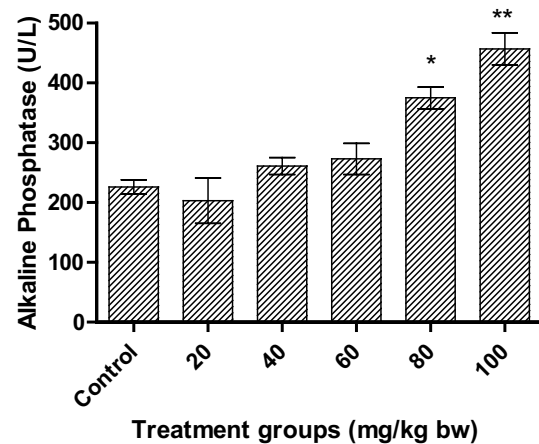
Table 3 Evaluation of various biochemical parameters after exposure to different concentrations of AgNP

	Dose (mg/kg bw)					
	0 (control)	20	40	60	80	100
ALB (g/dl)	2.82 ± 0.02	2.77 ± 0.04	2.68 ± 0.02	2.61 ± 0.03	2.58 ± 0.03	2.41 ± 0.01*
CHO (mg/dl)	105.26 ± 1.48	117.28 ± 1.73	126.56 ± 1.85	134.49 ± 1.48*	151.82 ± 1.93*	158.83 ± 1.84*
CRE (mg/dl)	0.82 ± 0.13	0.89 ± 0.14	0.92 ± 0.11	0.96 ± 0.14	1.01 ± 0.11	1.06 ± 0.10
GLU (mg/dl)	141.24 ± 6.39	148.39 ± 4.21	155.38 ± 3.82	164.92 ± 5.18	187.42 ± 4.48*	200.42 ± 4.29**
LDH (IU/l)	727.38 ± 18.39	702.56 ± 25.92	652.73 ± 14.08	593.92 ± 20.71	541.94 ± 16.32*	484.28 ± 32.96**
TP (g/dl)	6.46 ± 0.1	6.35 ± 0.08	6.24 ± 0.11	6.05 ± 0.14	5.98 ± 0.16	5.82 ± 0.17
IP (mg/dl)	6.82 ± 1.11	6.52 ± 1.39	6.07 ± 1.73	5.82 ± 1.04	5.69 ± 1.82	5.16 ± 0.93
TRG (mg/dl)	42.73 ± 4.21	44.29 ± 5.12	48.94 ± 5.25	52.92 ± 4.82	58.25 ± 2.02*	63.24 ± 5.22*
Na (mmol/l)	140.24 ± 1.83	140.85 ± 1.49	141.03 ± 1.38	141.22 ± 1.52	141.68 ± 1.30	142.04 ± 1.32
K (mmol/l)	4.08 ± 0.72	3.95 ± 0.53	3.88 ± 0.41	3.61 ± 0.72	3.48 ± 0.53	3.31 ± 0.24

*Significance of $p < 0.05$ **Significance of $p < 0.01$ **Fig. 5** Effect on total, direct, and indirect bilirubin in Wistar rats after treatment with AgNPs. Significant increase in total bilirubin was observed for 60, 80, and 100 mg/kg bw. Each datum represents the mean ± SD ($n = 5$)

significant increase in permeability, leading to uncontrolled transport through the plasma membrane and, finally, cell death (Garza-Ocañas et al. 2010). A significant increase in GLU, CHO, and TRG indicates hepatotoxicity. A significant increase has been reported earlier (De Jong et al. 2013; Kim et al. 2008; Lotfi et al. 2017). These studies have also indicated an alteration in liver enzymes also such as ALT, AST, and ALP. In addition, increase in CRE indicates impaired kidney function.

As depicted in Fig. 5, total, direct, and indirect bilirubin were analyzed. No significant change was observed for the doses 20 mg/kg bw and 40 mg/kg bw. For direct bilirubin, a significant increase ($p < 0.05$) was observed for 60, 80, and 100 mg/kg bw as compared to control. However, the total bilirubin was more significantly increased ($p < 0.01$) for 80 mg/kg bw and 100 mg/kg bw than for 60 mg/kg bw.

**Fig. 6** Effect on ALP in Wistar rats after treatment with AgNPs at different concentrations. Significant increase was observed for higher doses. Each datum represents the mean ± SD ($n = 5$)

It was also observed for higher doses that the total bilirubin was mostly conjugated (direct) bilirubin. When more than 50% of the total bilirubin is conjugated (direct) bilirubin, hepatocellular injury can be inferred. This suggests that hepatocellular injury may have occurred for higher doses. Magaye et al. have observed acute toxicity of nickel nanoparticles in Sprague–Dawley rats when treated with intravenous injection. They observed a significant increase in levels of total bilirubin and ALP leading to spleen injury (Magaye et al. 2014).

As depicted in Fig. 6, a significant increase in ALP was observed for higher doses only. At a dose of 100 mg/kg bw, the increase was more significant ($p < 0.01$) than for 80 mg/kg bw ($p < 0.05$). The level of ALP almost doubled

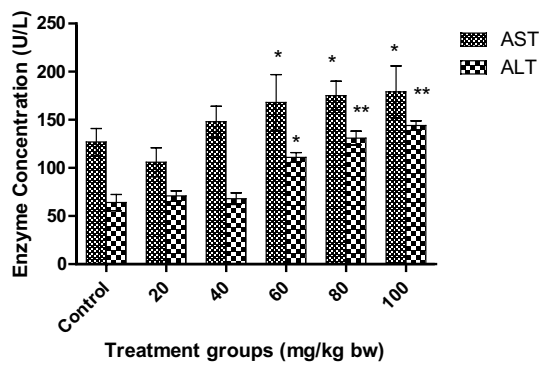


Fig. 7 Effect on AST and ALT in Wistar rats after treatment with AgNPs at different concentrations. Each datum represents the mean \pm SD ($n=5$)

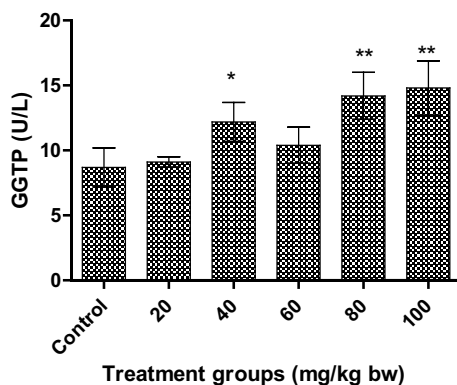


Fig. 8 Effect on GGTP in Wistar rats after treatment with AgNPs at different concentrations. Each datum represents the mean \pm SD ($n=5$)

for 100 mg/kg bw. Interestingly, there was no significant increase for 60 mg/kg bw, as was observed for total bilirubin.

In the present study, a significant increase in AST levels was observed for the higher and medium dose, that is, for 60, 80, and 100 mg/kg bw, as depicted in Fig. 7. Interestingly, the levels were significantly higher than the control ($p < 0.05$), but almost similar levels were obtained for 60, 80, and 100 mg/kg bw. The levels of AST increased from 127.2 ± 13.7 U/l of control to 179.3 ± 19.5 U/l at the treatment of 100 mg/kg bw. However, the levels of AST at 60, 80, and 100 mg/kg bw were 168.5 ± 29.1 U/l, 175.8 ± 15.8 U/l, and 179.3 ± 19.5 U/l, respectively, indicating no significant changes in these three doses. However, for ALT levels, more significant increase was observed ($p < 0.01$) for 80 and 100 mg/kg bw treatment dose than for 60 mg/kg bw ($p < 0.05$), as depicted in Fig. 7. The levels increased from 64.8 ± 8.4 U/l of control to 144.2 ± 4.8 U/l.

An increase in levels of GGTP was observed after 12 weeks repeated treatment with AgNPs. A significant increase ($p < 0.01$) was observed for the higher doses, 8.7 ± 1.5 U/l and 14.8 ± 2.1 U/l for 80 and 100 mg/kg bw,

respectively, as depicted in Fig. 8. Interestingly, a significant increase ($p < 0.05$) was observed for 40 mg/kg bw also, whereas no significant change was observed for other enzymes and protein at this treatment dose. In addition, no significant change was observed for the treatment dose at 60 mg/kg bw.

Elevated serum GGTP and ALP activity is related to liver diseases, biliary system, and pancreas, while ALT and AST are the indicator of hepatocellular level damages (Tiwari et al. 2011). AgNPs are reported to accumulate in renal tubular epithelial cells and hepatic cells and thus cause alteration in liver and kidney enzymes. However, the microparticles (323 nm) could not invade the blood stream or organ tissues. This indicates that AgNPs have size-dependent toxicity mechanism (Tang et al. 2009). As indicated in various in vitro studies, the major toxicity mechanism is oxidative stress. Inflammatory responses resulting from oxidative stress have been reported to be induced by AgNPs in rats. Park et al. have reported the increased production of cytokines and TGF- β after repeated oral administration of AgNP in mice (Park et al. 2010). Kim et al. carried out sub-chronic oral toxicity of AgNPs in rats. They observed NOAEL (no observable adverse effect level) at 30 mg/kg and LOAEL (lowest observable adverse effect level) at 125 mg/kg for AgNP of size 56 nm (Kim et al. 2010). However, at a similar size that is at 60 nm, we also observed an NOAEL at 30 mg/kg bw, but LOAEL was 60 mg/kg bw. This difference may be due to the different synthesis protocol followed.

Histopathology

To investigate the toxicity of AgNPs and the deposition within the cells, histopathology was performed on tissues from major organs. At the end of the study, rats were sacrificed and the tissues of lungs, liver, kidney, pancreas, and heart of the rats of higher treatment dose 100 mg/kg bw were analyzed. Mild congestion was observed in the lung tissue as compared to the control, as shown in Fig. 9a. Histopathological examinations by Sung et al. indicated that dose-dependent increases in lesions related to silver nanoparticle exposure, such as infiltrate mixed cell and chronic alveolar inflammation, including thickened alveolar walls and small granulomatous lesions upon exposure with prolonged inhalation to AgNPs (Sung et al. 2008). MNC (Mononuclear cell) infiltration and congestion was observed for liver tissue as compared to control (Fig. 9b). Particle deposition was also observed in the liver cells. As indicated from the figure, AgNP particle accumulation occurs mainly in liver and alteration in liver enzymes was also observed. Kim et al. observed the target organ for AgNP accumulation to be in liver (Kim et al. 2010).

Tubular degeneration and tubular dilation were observed in kidney tissue as compared to control (Fig. 9c). Due to

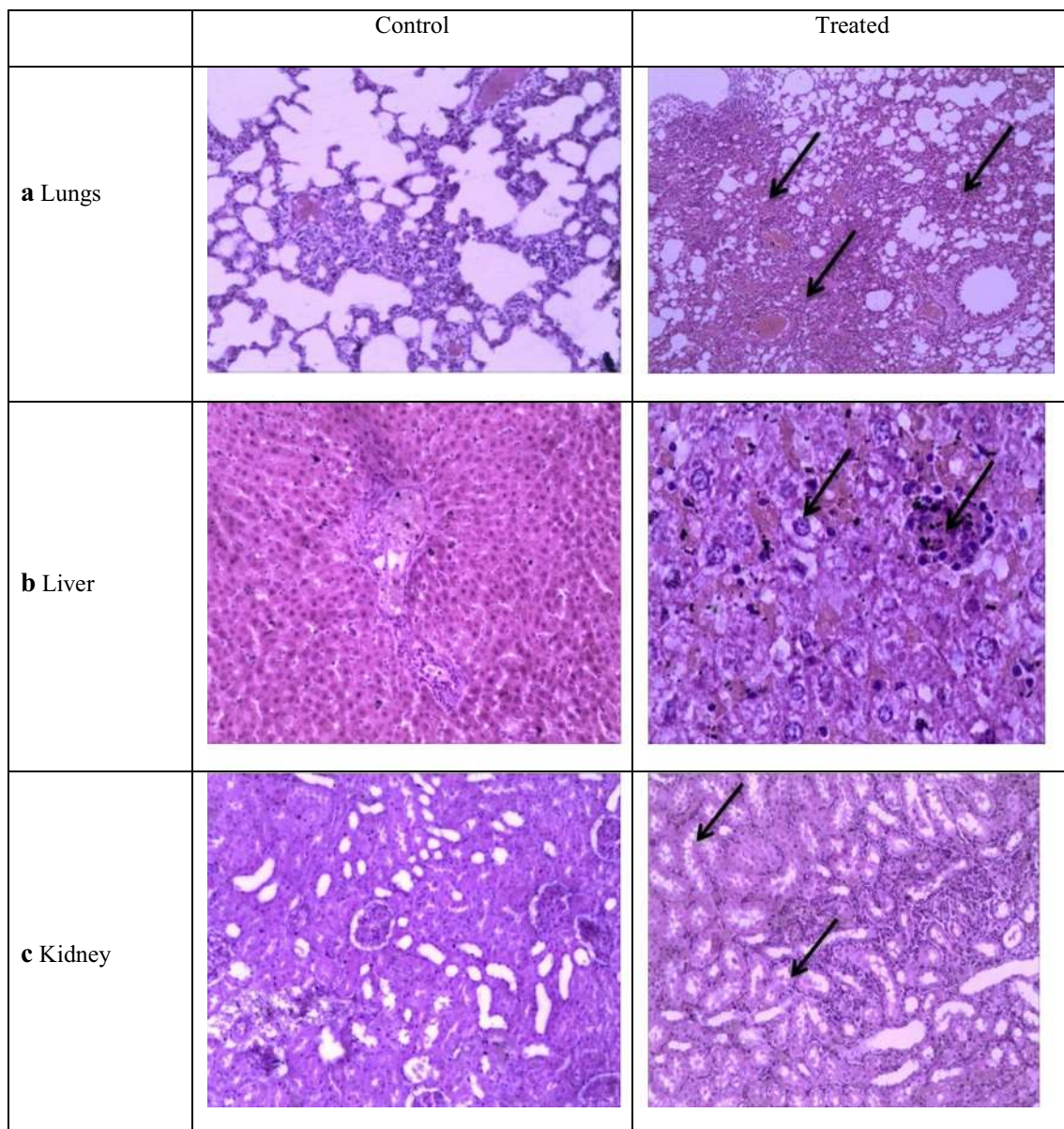


Fig. 9 Histopathology of **a** lungs, **b** liver, **c** kidney tissues—control and treated with AgNP. The tissues were stained with hematoxylin and eosin and observed for any disintegrity

particle deposition, the cells appear to be constricted. However, no abnormalities were observed for heart and pancreatic tissue. No severe damage was observed in these tissues and the cellular morphology and membrane integrity was maintained. AgNPs are reported.

Kim et al. observed a twofold higher accumulation in kidneys of female Fischer 344 rats than in males. The preferential accumulation sites were mainly due to disruption of the basement membrane of the glomerulus and renal

Table 4 Concentration of silver in different major organs as estimated by ICP-MS

	Lungs	Liver	Kidney	Heart	Pancreas
AgNP (μg of Ag/g of organ)	11 ± 0.1	36.3 ± 0.6	28 ± 0.3	–	0.8 ± 0.01

Each datum represents the mean \pm SD ($n=5$)

tubules, along with the adrenal capsule and cortex. The probable reason may be due to hormonal regulation. The kidneys are a target organ for several hormones, such as thyroid hormones and testosterone, with important physiological and pathological effects on the systemic and renal functions. Testosterone also has a stimulatory effect on several renal cellular functions, such as secretion, whereas female sexual hormones do not exhibit any apparent effect on secretion (Kim et al. 2009b).

Determination of silver concentrations in tissues

In the present study, the concentration of AgNP was determined by ICP-MS and is tabulated in Table 4. The concentration of AgNP was maximum in liver tissues than rest of the tissues examined. These results are in corroboration with the other results of our study. In addition, the previous studies also indicate the major target organ for AgNP toxicity to be liver. Hepatic toxicity and bile duct hyperplasia have been reported by the previous reports and also observed in our histopathology (Kim et al. 2008, 2010; Sung et al. 2009).

Conclusion

In this study, a concentration of 40 mg/kg bw was observed to be toxic in nature. It impaired liver and kidney functions as depicted from the enzyme levels. The LD₅₀ value was estimated to be more than 2000 mg/kg bw, as observed in acute toxicity studies. Particle deposition and congestion was observed in major organs. However, heart and pancreas tissue were not affected even by the higher doses. Thus, AgNPs are not completely eliminated from the body and these trapped AgNPs in major organs can cause further damage. On the basis of the data obtained in this study, it is concluded that up to 40 mg/kg is a safe dose of AgNPs and is recommended for use. However, a long-term dosage study can be done to understand the adverse effects of AgNP consumption.

Acknowledgements SR is acknowledging Department of Biotechnology, Ministry of Science and Technology (DBT, India) for the funding with Grant number—BT/PR10414/PFN/20/961/2014. SR is acknowledging Veer Kunwar Singh Memorial Trust, Chapra, Bihar, India, for partial support—VKSM/ST/SN/NFNA/0011.

Compliance with ethical standards

Conflict of interest Authors are declaring no conflicts of interest.

References

- Akter M, Sikder MT, Rahman MM, Ullah AKMA, Hossain KFB, Banik S, Kurasaki M (2018) A systematic review on silver nanoparticles-induced cytotoxicity: physicochemical properties and perspectives. *J Adv Res* 9:1–16
- Alarifi S, Ali H, Alkahtani S, Alessia MS (2017) Regulation of apoptosis through bcl-2/bax proteins expression and DNA damage by nano-sized gadolinium oxide. *Int J Nanomed*. <https://doi.org/10.2147/IJN.S139326>
- Chakraborty B, Pal R, Ali M, Singh LM, Rahman S, Ghosh D, Kumar S, Sengupta M (2016) Immunomodulatory properties of silver nanoparticles contribute to anticancer strategy for murine fibrosarcoma. *Cell Mol Immunol*. <https://doi.org/10.1038/cmi.2015.05>
- Chang ALS, Khosravi V, Egbert B (2006) A case of argyria after colloidal silver ingestion. *J Cutan Pathol* 33(12):809–811
- Chen LQ, Fang L, Ling J, Ding CZ, Kang B, Huang CZ (2015) Nanotoxicity of silver nanoparticles to red blood cells: size dependent adsorption, uptake, and hemolytic activity. *Chem Res Toxicol* 28(3):501–509
- Daniel SCGK, Tharmaraj V, Sironmani TA, Pitchumani K (2010) Toxicity and immunological activity of silver nanoparticles. *Appl Clay Sci* 48(4):547–551
- Dasgupta N, Ramalingam C (2016) Silver nanoparticle antimicrobial activity explained by membrane rupture and reactive oxygen generation. *Environ Chem Lett* 14(4):477–485. <https://doi.org/10.1007/s10311-016-0583-1>
- Dasgupta N, Ranjan S, Rajendran B, Manickam V, Ramalingam C, Avadhani G, Ashutosh K (2016) Thermal co-reduction approach to vary size of silver nanoparticle: its microbial and cellular toxicology. *Environ Sci Pollut Res* 23:4149–4163
- De Jong WH, Van Der Ven LTM, Sleijffers A, Park MVDZ, Jansen EHJM, Van Loveren H, Vandebriel RJ (2013) Systemic and immunotoxicity of silver nanoparticles in an intravenous 28 days repeated dose toxicity study in rats. *Biomaterials* 34(33):8333–8343
- Dobrzyńska MM, Gajowik A, Radzikowska J, Lankoff A, Duśińska M, Kruszewski M (2014) Genotoxicity of silver and titanium dioxide nanoparticles in bone marrow cells of rats in vivo. *Toxicology* 315:86–91. <https://doi.org/10.1016/j.tox.2013.11.012>
- El Badawy AM, Silva RG, Morris B, Scheckel KG, Suidan MT, Tolaymat TM (2010) Surface charge-dependent toxicity of silver nanoparticles. *Environ Sci Technol* 45(1):283–287
- Espinosa-Cristobal LF, Martinez-Castanon GA, Loyola-Rodriguez JP, Patino-Marin N, Reyes-Macias JF, Vargas-Morales JM, Ruiz F (2013) Toxicity, distribution, and accumulation of silver nanoparticles in Wistar rats. *J Nanopart Res* 15(6):1702
- Gaillet S, Rouanet J-M (2015) Silver nanoparticles: their potential toxic effects after oral exposure and underlying mechanisms—a review. *Food Chem Toxicol* 77:58–63
- Garza-Ocañas L, Ferrer DA, Burt J, Diaz-Torres LA, Cabrera MR, Rodríguez VT, Jose-Yacaman M (2010) Biodistribution and long-term fate of silver nanoparticles functionalized with bovine serum albumin in rats. *Metallomics* 2(3):204–210
- Gnanadhas DP, Ben Thomas M, Thomas R, Raichur AM, Chakravorty D (2013) Interaction of silver nanoparticles with serum proteins affects their antimicrobial activity in vivo. In: Antimicrobial agents and chemotherapy, 1752 St. N, N.W., Washington, DC. <https://doi.org/10.1128/AAC.00152-13>
- Hadrup N, Loeschner K, Bergström A, Wilcks A, Gao X, Vogel U, Mortensen A (2012) Subacute oral toxicity investigation of nanoparticulate and ionic silver in rats. *Arch Toxicol* 86(4):543–551
- Kim YS, Kim JS, Cho HS, Rha DS, Kim JM, Park JD et al (2008) Twenty-eight-day oral toxicity, genotoxicity, and gender-related

- tissue distribution of silver nanoparticles in Sprague-Dawley rats. *Inhal Toxicol* 20(6):575–583
- Kim S, Choi JE, Choi J, Chung K-H, Park K, Yi J, Ryu D-Y (2009a) Oxidative stress-dependent toxicity of silver nanoparticles in human hepatoma cells. *Toxicol In Vitro* 23(6):1076–1084
- Kim W-Y, Kim J, Park JD, Ryu HY, Yu IJ (2009b) Histological study of gender differences in accumulation of silver nanoparticles in kidneys of Fischer 344 rats. *J Toxicol Environ Health Part A* 72(21–22):1279–1284. <https://doi.org/10.1080/15287390903212287>
- Kim YS, Song MY, Park JD, Song KS, Ryu HR, Chung YH, Yu IJ (2010) Subchronic oral toxicity of silver nanoparticles. *Part Fibre Toxicol* 7(1):20. <https://doi.org/10.1186/1743-8977-7-20>
- Lankveld DPK, Oomen AG, Krystek P, Neigh A, de Jong AT, Noorlander CW, De Jong WH (2010) The kinetics of the tissue distribution of silver nanoparticles of different sizes. *Biomaterials* 31(32):8350–8361. <https://doi.org/10.1016/j.biomaterials.2010.07.045>
- Lappas CM (2015) The immunomodulatory effects of titanium dioxide and silver nanoparticles. *Food Chem Toxicol* 85:78–83
- Loeschner K, Hadrup N, Qvortrup K, Larsen A, Gao X, Vogel U, Larsen EH (2011) Distribution of silver in rats following 28 days of repeated oral exposure to silver nanoparticles or silver acetate. *Part Fibre Toxicol* 8(1):18
- Lotfi A, Aghdam EG, Narimani-Rad M (2017) Effect of chemically-synthesized silver nanoparticles (ag-np) on glycemic and lipidemic status in rat model. In: Badnjevic A (ed) *CMBEBIH 2017: proceedings of the international conference on medical and biological engineering 2017*. Springer, Singapore, pp 158–163. https://doi.org/10.1007/978-981-10-4166-2_25
- Ma X, Geiser-Lee J, Deng Y, Kolmakov A (2010) Interactions between engineered nanoparticles (ENPs) and plants: phytotoxicity, uptake and accumulation. *Sci Total Environ* 408(16):3053–3061
- Magaye RR, Yue X, Zou B, Shi H, Yu H, Liu K, Zhao J (2014) Acute toxicity of nickel nanoparticles in rats after intravenous injection. *Int J Nanomed*. <https://doi.org/10.2147/IJN.S56212>
- Maneewattanapinyo P, Banlunara W, Thammacharoen C, Ekgasit S, Kaewamatawong T (2011) An evaluation of acute toxicity of colloidal silver nanoparticles. *J Vet Med Sci* 73(11):1417–1423
- Nguyen KC, Seligy VL, Massarsky A, Moon TW, Rippstein P, Tan J, Tayabali AF (2013) Comparison of toxicity of uncoated and coated silver nanoparticles. *J Phys Conf Ser* 429:12025
- Park E-J, Bae E, Yi J, Kim Y, Choi K, Lee SH, Park K (2010) Repeated-dose toxicity and inflammatory responses in mice by oral administration of silver nanoparticles. *Environ Toxicol Pharmacol* 30(2):162–168
- Park MVDZ, Neigh AM, Vermeulen JP, de la Fonteyne LJJ, Verharen HW, Briedé JJ, de Jong WH (2011) The effect of particle size on the cytotoxicity, inflammation, developmental toxicity and genotoxicity of silver nanoparticles. *Biomaterials* 32(36):9810–9817
- Pindřáková L, Kašpárková V, Kejlová K, Dvořáková M, Krsek D, Jírová D, Kašparová L (2017) Behaviour of silver nanoparticles in simulated saliva and gastrointestinal fluids. *Int J Pharm* 527(1):12–20. <https://doi.org/10.1016/j.ijpharm.2017.05.026>
- Ranganathan A, Hindupur R, Vallikannan B (2016) Biocompatible lutein-polymer-lipid nanocapsules: acute and subacute toxicity and bioavailability in mice. *Mater Sci Eng C* 69:1318–1327. <https://doi.org/10.1016/j.msec.2016.08.029>
- Shahare B, Yashpal M, Gajendra (2013) Toxic effects of repeated oral exposure of silver nanoparticles on small intestine mucosa of mice. *Toxicol Mech Methods* 23(3):161–167
- Srivastava M, Singh S, Self WT (2012) Exposure to silver nanoparticles inhibits selenoprotein synthesis and the activity of thioredoxin reductase. *Environ Health Perspect* 120(1):56–61. <https://doi.org/10.1289/ehp.1103928>
- Stebounova LV, Adamcakova-Dodd A, Kim JS, Park H, O'Shaughnessy TP, Grassian VH, Thorne PS (2011) Nanosilver induces minimal lung toxicity or inflammation in a subacute murine inhalation model. *Part Fibre Toxicol* 8(1):5
- Sung JH, Ji JH, Yoon JU, Kim DS, Song MY, Jeong J, Yu IJ (2008) Lung function changes in Sprague-Dawley rats after prolonged inhalation exposure to silver nanoparticles. *Inhal Toxicol* 20(6):567–574. <https://doi.org/10.1080/08958370701874671>
- Sung JH, Ji JH, Park JD, Yoon JU, Kim DS, Jeon KS, Yu IJ (2009) Subchronic inhalation toxicity of silver nanoparticles. *Toxicol Sci*. <https://doi.org/10.1093/toxsci/kfn246>
- Tang J, Xiong L, Wang S, Wang J, Liu L, Li J, Xi T (2009) Distribution, translocation and accumulation of silver nanoparticles in rats. *J Nanosci Nanotechnol* 9(8):4924–4932
- Tang J, Xiong L, Zhou G, Wang S, Wang J, Liu L et al (2010) Silver nanoparticles crossing through and distribution in the blood-brain barrier in vitro. *J Nanosci Nanotechnol* 10(10):6313–6317
- Tiwari DK, Jin T, Behari J (2011) Dose-dependent in-vivo toxicity assessment of silver nanoparticle in Wistar rats. *Toxicol Mech Methods* 21(1):13–24
- van der Zande M, Vandebriel RJ, Van Doren E, Kramer E, Herrera Rivera Z, Serrano-Rojero CS et al (2012) Distribution, elimination, and toxicity of silver nanoparticles and silver ions in rats after 28-day oral exposure. *ACS Nano* 6(8):7427–7442
- Völker C, Oetken M, Oehlmann J (2013) The biological effects and possible modes of action of nanosilver. In: Whitacre D (ed) *Reviews of environmental contamination and toxicology*, vol 223. Springer, New York, NY, pp 81–106. https://doi.org/10.1007/978-1-4614-5577-6_4
- Xue Y, Zhang S, Huang Y, Zhang T, Liu X, Hu Y, Tang M (2012) Acute toxic effects and gender-related biokinetics of silver nanoparticles following an intravenous injection in mice. *J Appl Toxicol* 32(11):890–899
- Yun J-W, Kim S-H, You J-R, Kim WH, Jang J-J, Min S-K, Che J-H (2015) Comparative toxicity of silicon dioxide, silver and iron oxide nanoparticles after repeated oral administration to rats. *J Appl Toxicol* 35(6):681–693. <https://doi.org/10.1002/jat.3125>